

1 Running title: The function of *BOS1*

2 **BOS1 is a positive regulator of wounding induced cell death and plant**
3 **susceptibility to *Botrytis***

4 Fuqiang Cui^{1, #, *,}, Xiaoxiao Li^{1, #}, Wenwu Wu^{1, #}, Wenbo Luo¹, Ying Wu¹, Mikael
5 Brosché², and Kirk Overmyer²

¹ State Key Laboratory of Subtropical Silviculture, Zhejiang A&F University, Lin'an 311300, Hangzhou, China.

² Organismal and Evolutionary Biology Research Program, Faculty of Biological and Environmental Sciences, and the Viikki Plant Science Centre, University of Helsinki, P.O. Box 65 (Viikinkaari 1), FI-00014 Helsinki, Finland.

These authors contributed equally.

* **Address correspondence to:**

Fuqiang Cui, Zhejiang A&F University, China.

email: fuqiang.cui@gmail.com, phone: +86 18958073673.

State Key Laboratory of Subtropical Silviculture, Zhejiang A&F University, Lin'an 311300, Hangzhou, China.

6

7

8 **Abstract**

9 Programmed cell death (PCD) is required for many aspects of plant biology,
10 including stress responses, immunity, and plant development including root and
11 flower development. Our understanding of PCD regulation is incomplete,
12 especially concerning regulators involved in multiple divergent processes. The
13 *botrytis-susceptible1* (*bos1*) mutant is one of the genotypes most susceptible to
14 *Botrytis cinerea* (*Botrytis*) and has revealed the role of *BOS1* in cell death
15 propagation during plant responses to wounding. The *bos1-1* allele harbours a T-
16 DNA located in the 5'UTR upstream from the start codon that results in elevated
17 *BOS1* transcript levels. Here, we resequenced the *bos1-1* genome and found a
18 *MAS* promoter at the ends of the T-DNAs. Expression of the *BOS1* gene under
19 control of the *MAS* promoter conferred the characteristic *bos1-1 Botrytis*-
20 sensitivity and wounding phenotypes in wildtype plants. We used Crispr-Cas9 to
21 create new *bos1* alleles that disrupt exons. These lines lacked the typical *bos1-1*
22 wounding and *Botrytis* phenotypes, but exhibited reduced fertility, as previously
23 observed in other *bos1* T-DNA alleles. With multiple overexpression lines of
24 *BOS1*, we demonstrate that *BOS1* is involved in regulation of cell death
25 propagation in a dosage dependent manner. Our data support that *bos1-1* is a
26 gain-of-function mutant and that *BOS1* acts as a positive regulator of wounding
27 and *Botrytis*-induced PCD. Taken together these finding suggest that *BOS1*
28 function in both fertility and *Botrytis* response could be unified under cell death
29 control.

30

31

32

33 Introduction

34 Programmed cell death (PCD) is a finely tuned process, which occurs for
35 example during plant-pathogen interactions and plant development, and has
36 three stages including cell death initiation, propagation, and containment
37 (McCabe, 2013; Van Hautegeem et al., 2015). Many PCD regulators have been
38 identified in *Arabidopsis thaliana* (*Arabidopsis*) from lesion mimic mutants that
39 spontaneously develop cell death (Lorrain et al., 2003; Bruggeman et al., 2015).
40 A separate class of regulators have been recognized from so called propagation
41 class lesion mimic mutants, in which uncontained or “runaway” spreading cell
42 death that can consume the entire leaf is observed once cell death is initiated
43 (Lorrain et al., 2003). Although these have been crucial to understand the
44 processes involved in regulation of cell death, for example the central role of
45 several plant hormones (Bruggeman et al., 2015), our understanding of the
46 signals leading to propagation and containment of cell death remains incomplete.
47 Uncontained abscisic-acid dependent PCD propagation was found in *botrytis-*
48 *susceptible1-1* (*bos1-1*; Cui et al., 2013), a mutant allele of *BOS1/MYB108*
49 (At3g06490; Mengiste et al. 2003). PCD propagation was enhanced in *bos1-1*
50 once death was initiated by pathogen infection or simply mechanical injury (Cui
51 et al., 2013, 2019). Mechanical injury results in local cell death immediately
52 adjacent to the wound in order to re-establish the integument (McCabe, 2013;
53 Cui et al., 2013; Bostock and Stermer, 1989; Iakimova and Woltering, 2018). This
54 wound-induced cell death response allows controlled PCD development at a
55 fixed site, which makes wounding of *bos1-1* an attractive experimental system for
56 studies on PCD propagation (McCabe, 2013). *BOS1* is a R2R3 MYB
57 transcription factor, which was first functionally characterized with the *bos1-1*
58 mutant, based on its striking susceptibility to the necrotrophic fungal pathogen
59 *Botrytis cinerea*, in the seminal paper by Mengiste et al. (2003). Subsequently,
60 *BOS1* has been recognized as a key gene involved in plant-pathogen
61 interactions, and *bos1-1* has helped to reveal the important role of cell death in
62 susceptibility to necrotrophic fungi (Kraepiel et al., 2011; Cui et al., 2013, 2019).
63 The *bos1-1* allele was genetically characterized as a recessive loss-of-function

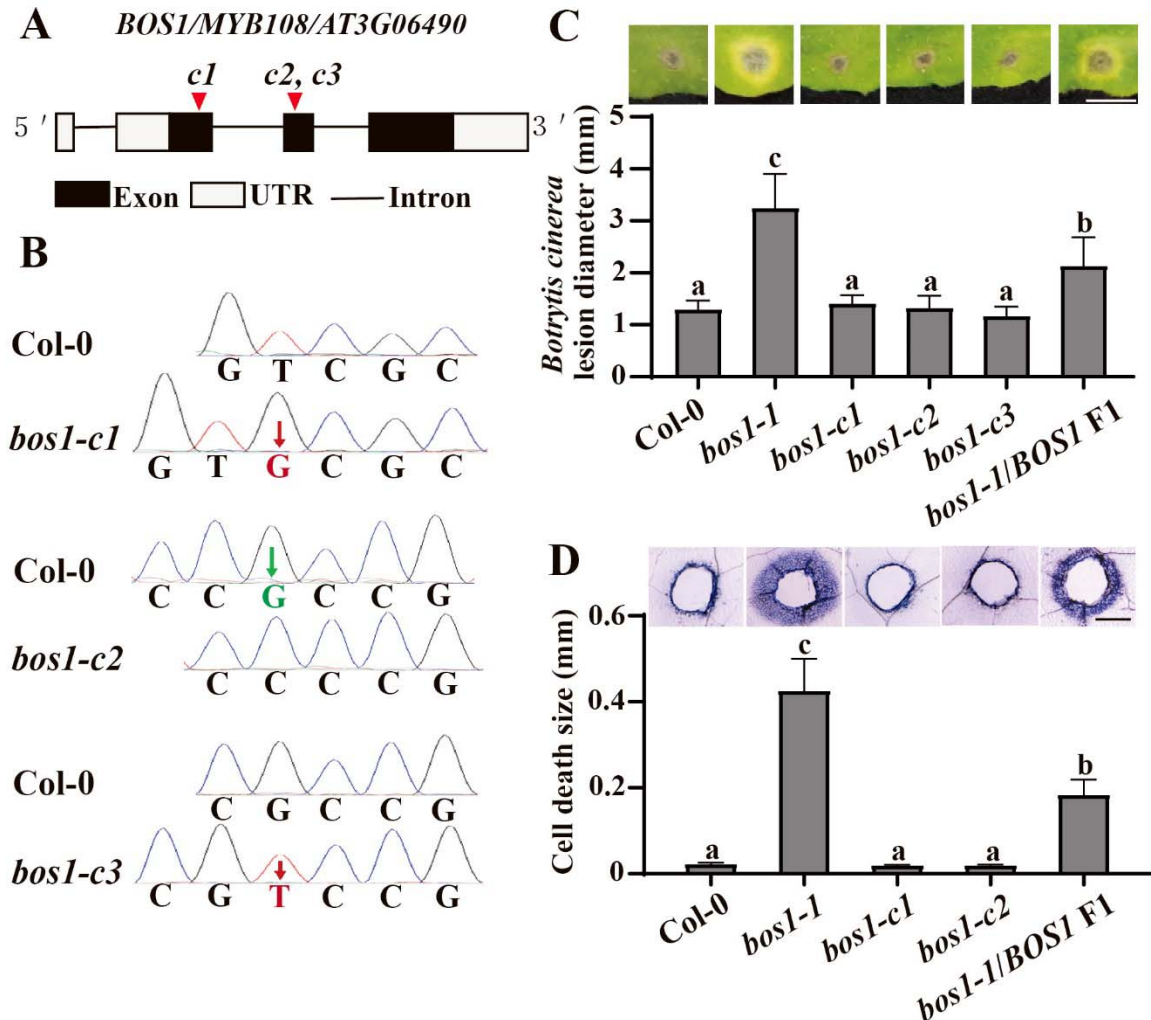
64 mutant, although the T-DNA insertion is located in the 5'UTR upstream from the
65 start codon and results in abnormally high expression of *BOS1* (Mengiste et al.,
66 2003).

67 PCD is also indispensable for plant development, including reproductive
68 development where PCD is required for both proper development and release of
69 pollen (Mandaokar and Browse, 2009; Daneva et al., 2016; Xu et al., 2019). One
70 open question in plant PCD research is to which extent pathogen activated and
71 developmental PCD overlap in regulatory mechanisms and execution (Huysmans
72 et al., 2017). *BOS1* functions in both plant stress responses and development
73 (Mandaokar and Browse, 2009; Kraepiel et al., 2011; Cui et al., 2013; Xu et al.,
74 2019; Cui et al., 2019). *BOS1* can be ubiquitinated by BOTRYTIS
75 SUSCEPTIBLE1 INTERACTOR (BOI), an E3 ligase that attenuates stress
76 induced cell death in plants (Luo et al., 2010). Three mutant alleles with T-DNA
77 insertions in the first intron were used to study the role of *BOS1/MYB108* in
78 anther development (Mandaokar and Browse, 2009). The mutants displayed
79 reduced male fertility, lower pollen viability, and delayed anther dehiscence.
80 However, the stress response of these alleles remains untested. As different
81 *bos1* alleles were used in the study of pathogen versus developmental PCD,
82 there is a lack of information to which extent this transcription factor could act in
83 both types of cell death. Further, the existing mutants for *bos1* are either intron
84 insertions (Mandaokar and Browse, 2009) or a 5'-UTR insertion (*bos1-1*;
85 Mengiste et al., 2003), which makes interpretation of *BOS1* function in cell death
86 control unclear. Here we generated new *bos1* exon mutant alleles and present
87 evidence that this transcription factor is a positive regulator of cell death, in
88 contrast to the roles previously assigned to *BOS1*.

89

90 **Results**

91



92

93 **Figure 1. New *bos1* alleles created with Crispr-Cas9 did not exhibit *bos1-1* phenotypes.**

94 **(A)** Schematic diagram of the new *bos1* insertion and deletion alleles. The guide RNA (gRNA)
95 positions are indicated with red triangles and the new *bos1* alleles made by CRISPR were
96 designated as *c1*, *c2* and *c3*.

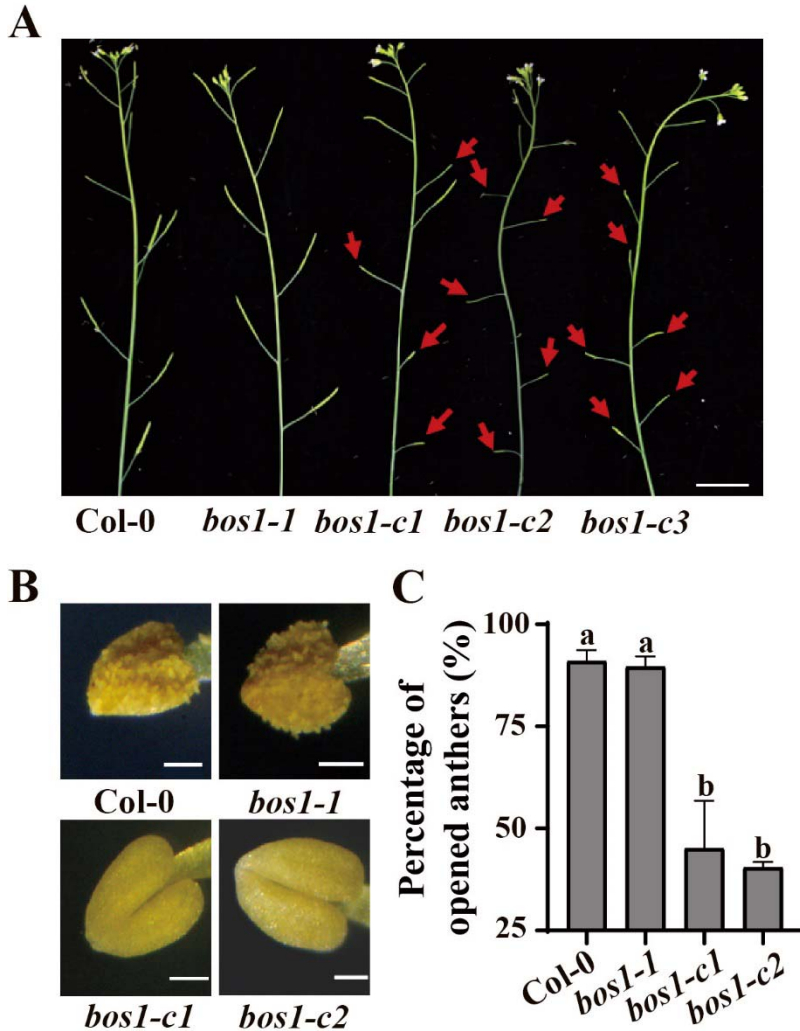
97 **(B)** Genome editing induced changes in the indicated mutants. Single base insertions (red
98 characters) and deletion (green characters) were detected with Sanger sequencing.

99 **(C)** Disease symptoms and lesion sizes induced by inoculation with *Botrytis cinerea*. Droplets of
100 conidia suspension ($3 \mu\text{l}$, 2×10^5 spores ml^{-1}) were inoculated on fully expanded leaves of the
101 indicated genotypes. Symptoms were photographed at three days post inoculation. Lesion sizes
102 were measured in ImageJ and statistically analysed with one-way ANOVA (three independent
103 biological replicates; $n=24$ in total). Scale bar=0.5 cm.

104 **(D)** Wound induced cell-death spread. Leaves punctured with a toothpick were subjected to
105 trypan blue staining to visualize dead tissue at four days post wounding. Representative pictures
106 are shown to illustrate the dead tissues around the wounds. The extent of cell death spread
107 was measured from the edge of the wound to the outer frontier of spreading cell death. These
108 experiments were performed three times with similar results ($n=24$ in total). Scale bar=0.5 mm.

109 ***Botrytis* and wounding response in new *bos1* Crispr alleles**

110 Genome editing allows the generation of desired mutants (Jiang et al., 2013;
111 Xing et al., 2014). We used CRISPR-Cas9 to create three *BOS1* loss-of-function
112 alleles, targeting the first and second exons (*bos1-c1* to *-c3*; Fig. 1A). These
113 mutations caused frame-shifts resulting in truncated proteins (Fig. 1B). None of
114 these alleles exhibited the characteristic *bos1-1* phenotypes seen with *Botrytis*
115 infection or wounding treatments. *Botrytis*-induced lesion sizes and wound-
116 induced cell death spread in these mutants were similar to wildtype (Fig. 1C and
117 D). This suggested that *bos1-1* may be not a true loss-of-function mutant of
118 *BOS1*. To confirm this hypothesis, we generated the heterozygous mutant *bos1-*
119 *1/BOS1* by a cross between *bos1-1* and wildtype. Upon wounding and *Botrytis*
120 treatments, *bos1-1/BOS1* exhibited intermediate phenotypes between wildtype
121 and the *bos1-1* homozygous mutant; both the extent of wounding-induced
122 runaway cell death and the size of *Botrytis*-induced lesions in *bos1-1/BOS1* were
123 significantly larger than wildtype but smaller than in *bos1-1* (Fig. 1C and D).
124 Further, we tested the distribution of *Botrytis*- and wounding-induced phenotypes
125 in a F₂ population derived from a confirmed *bos1-1/BOS1* heterozygote F₁
126 individual. These phenotyped F₂ populations revealed a 1:2:1 segregation ratio,
127 fitting the model where *bos1-1* is a co-dominant gain-of-function allele; in which
128 one quarter exhibited *bos1-1* symptoms; one half had intermediate phenotypes,
129 similar to *bos1-1/BOS1*; and one quarter had wild type characteristics
130 (Supplemental Fig. S1). Plants of one replicate were genotyped, which confirmed
131 that the plants exhibiting enhanced *Botrytis*-induced lesion size were *bos1-1*
132 homozygotes while the population exhibiting intermediate sized lesions were
133 *bos1-1/BOS1* heterozygotes (Supplemental Fig. S1). The genetics of both the F₁
134 and F₂ generations supports that *bos1-1* is a co-dominant gain-of-function mutant.



135

136 **Figure 2. Crispr *bos1* knock-out lines were impaired in pollen release.**

137 **(A)** The *bos1* alleles created with Crispr-Cas9 resulted in impaired fertility. Red arrows indicate
138 siliques with reduced seed production. Delayed flower senescence is also apparent in the *bos1*
139 Crispr-Cas9 alleles. Bar = 1 cm.

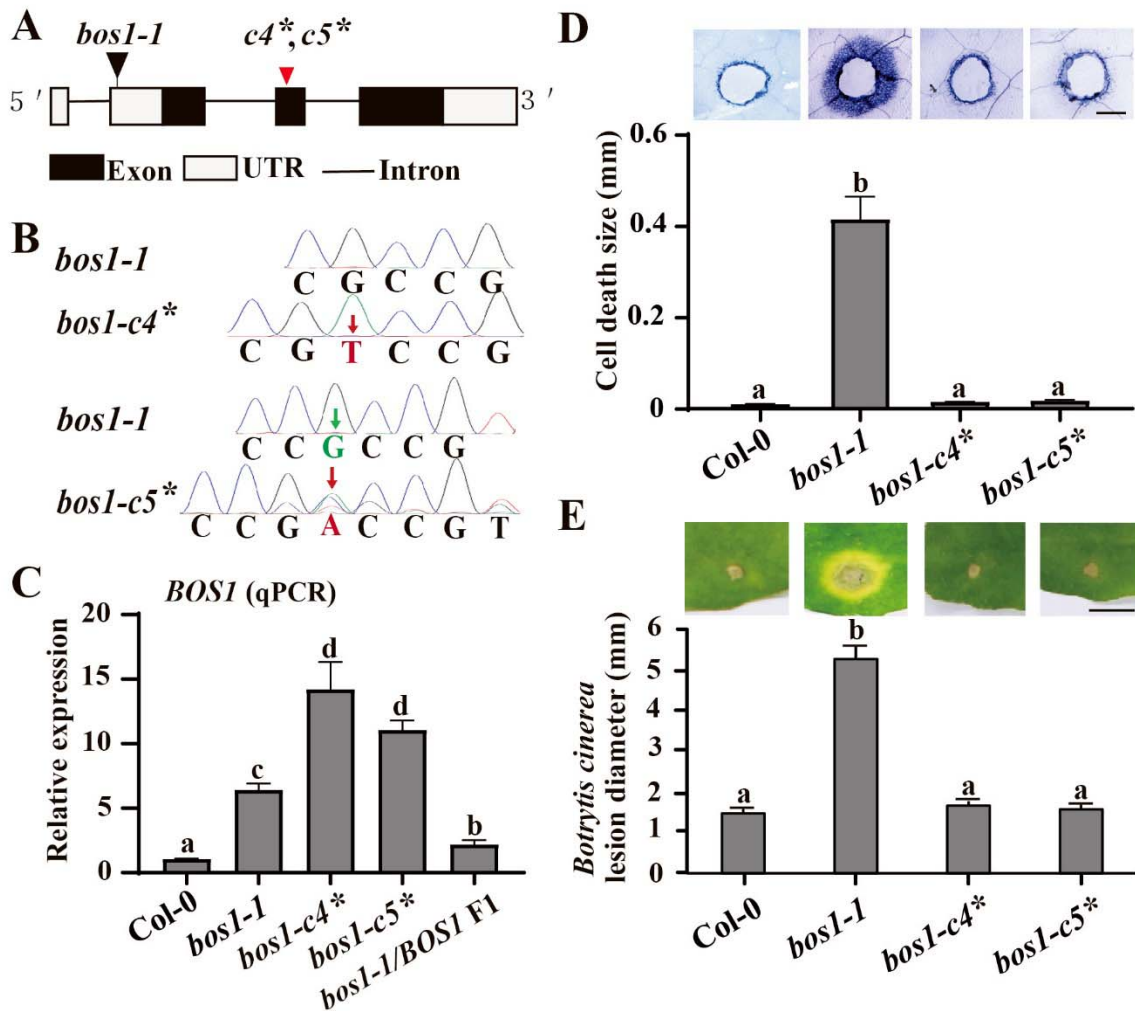
140 **(B)** Anthers of the Crispr-Cas9 knock-out alleles of *bos1* exhibited delayed dehiscence. Anthers
141 were detached from flowers at the same developmental stage (floral stage 14). Bar = 50 μ m.

142 **(C)** The percentage of anthers that have undergone dehiscence in the indicated genotypes. Ten
143 flowers of each genotype at the same developmental-stage were measured. The experiment was
144 repeated twice with similar results and one representative experiment is shown. Letters above
145 bars indicate significant differences between groups (one-way ANOVA, $P \leq 0.05$).

146 **Crispr *bos1* alleles are impaired in fertility**

147 The CRISPR knock-out lines exhibited strong deficiencies in fertility, which was
148 observed as the number of siliques with reduced size and a delay in flower

149 senescence (Fig. 2A). This finding is consistent with the reduced fertility
 150 phenotypes of mutants with T-DNA in the introns of *BOS1* (Xu et al., 2019;
 151 Mandaokar and Browse, 2009). Previous studies suggested that the impaired
 152 fertility of *bos1* intron T-DNA alleles was due to deficient or delayed pollen
 153 release, as their anthers were mostly still closed (Xu et al., 2019). We examined
 154 the anthers of the new CRISPR knock-out alleles and found the same phenotype.
 155 Pollen release was significantly reduced or delayed in comparison to wild type
 156 (Fig. 2B and C). In contrast, *bos1-1* did not exhibit any phenotypes in fertility and
 157 anther dehiscence (Fig. 2). The phenotypic similarity between our CRISPR
 158 knock-out lines and the previously used *BOS1* intron T-DNA alleles further
 159 support that *bos1-1* is not a loss-of-function mutant of *BOS1*.



160

161 **Figure 3. The *bos1-1* phenotypes were abolished by introduction of exon disrupting alleles**
162 **in *BOS1* with Crispr-Cas9.**

163 **(A)** Schematic diagram of the new intragenic double mutants *bos1-c4** and *-c5** created with
164 CRISPR-Cas9 in the *bos1-1* background, incorporating both the T-DNA insertions of *bos1-1* and
165 frame-shifts in the second exon of *BOS1*. Black triangle indicates the T-DNA of *bos1-1*. Red
166 triangle indicates the start of the frame-shifts of *bos1-c4** and *bos1-c5** (*c4**, *c5**).

167 **(B)** Single base insertions (red characters) and deletion (green characters) were detected with
168 Sanger sequencing. The thymidine nucleotide insertion in *bos1-c4** is homozygous, while in
169 *bos1-c5** there are two changes, an insertion of an adenine nucleotide and a deletion of a
170 guanine nucleotide.

171 **(C)** Relative expression of *BOS1* in the indicated genotypes. Fully expanded leaves of 24-day-old
172 plants were used for qPCR. Three biological replicates exhibited the same trends and one
173 representative is shown.

174 **(D)** Wounding induced cell-death spread was visualized with trypan blue staining. Representative
175 pictures are shown to illustrate the dead tissues around the toothpick-puncture wounds. These
176 experiments were performed three times with similar results ($n=24$ in total). Scale bar=0.5 mm.

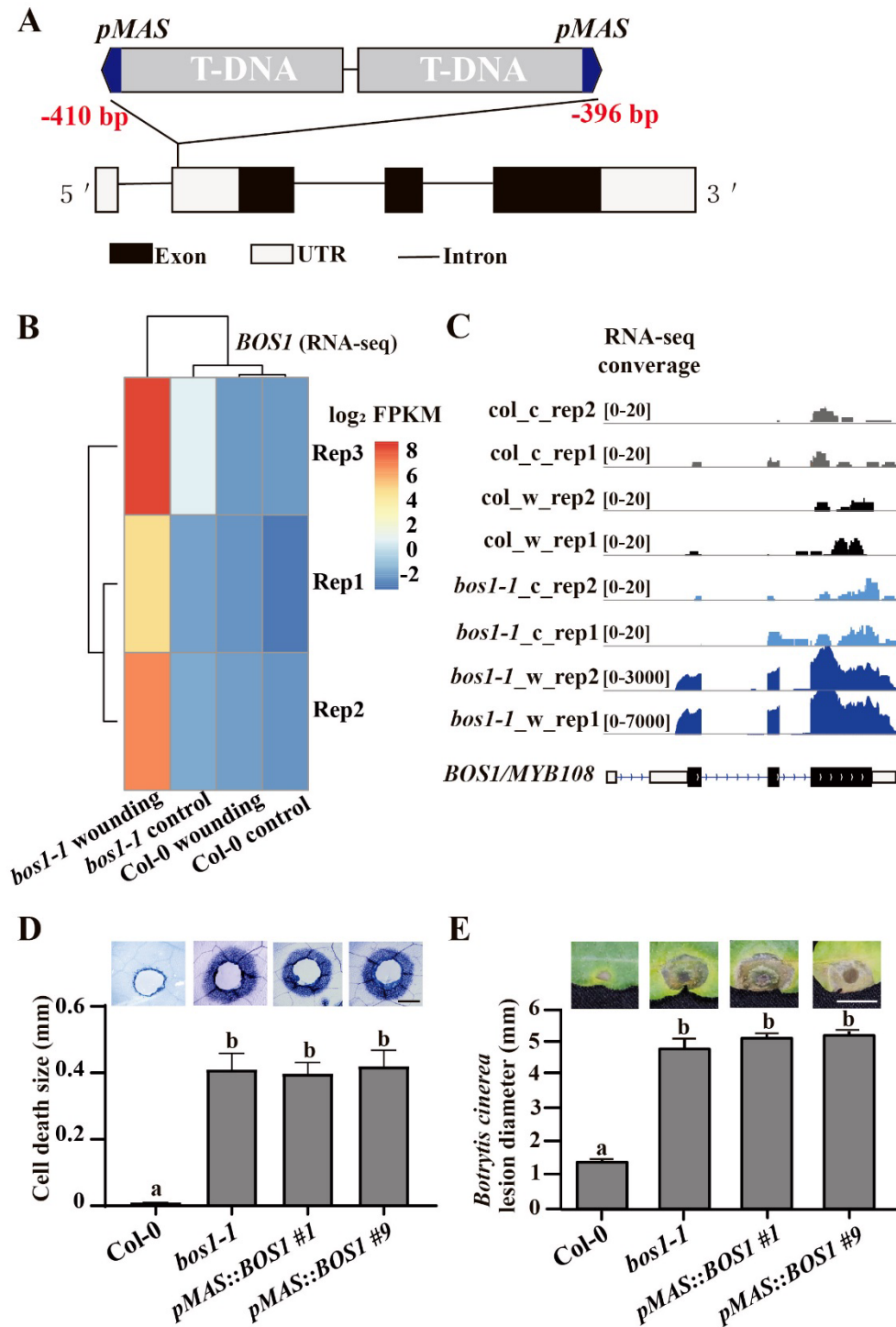
177 **(E).** *Botrytis* induced lesion sizes in the indicated genotype. Statistical analysis was performed
178 with one-way ANOVA (5 independent biological replicates; $n=72$ in total). All error bars represent
179 the SE of means. Letters above the bars indicated significance groups ($P<0.05$, linear mixed
180 model). Scale bar=0.5 cm.

181 **The *bos1-1* allele is a gain-of-function due to increased *BOS1* transcript**
182 **levels**

183 T-DNA insertions can result in genome structure changes or have epigenomic
184 impacts, which may contribute to the phenotypes independent of the T-DNA
185 insertion (Jupe et al., 2019). To comprehensively assess the genomic changes in
186 *bos1-1*, we performed Nanopore genome re-sequencing (Brown and Clarke,
187 2016). This analysis identified 1173 structural variations, including larger
188 rearrangements (>1000 bp), 13 insertions, 16 deletions, 19 duplications and 24
189 inversions, while no mutations were detected in the open reading frame of *BOS1*
190 (Supplemental Table S1). Considering the work required to assess the potential
191 role of these changes in the *bos1-1* phenotypes, we first used a strategy to test
192 the effect of additional exon disrupting mutations in the *bos1-1* background to
193 probe whether the *bos1-1* phenotypes were caused by increased *BOS1*
194 transcriptional levels. With Crispr-Cas9 we introduced a second mutation in exon
195 2 of *BOS1* in the *bos1-1* mutant background (Fig. 3A). These intragenic double
196 mutant alleles were assigned the designations *bos1-c4** and *bos1-c5** (*

197 indicates that the allele is an intragenic double mutant in *bos1-1* background).
198 Frame-shifts disrupting *BOS1* exon 2 were detected in these intragenic double
199 mutants (Fig. 3B). These second mutations did not attenuate the high *BOS1*
200 transcript levels seen in *bos1-1*, as *BOS1* transcript accumulation remained high
201 in *bos1-c4** and *bos1-c5** (Fig. 3C). The characteristic *bos1-1* phenotypes were
202 abolished in these lines: spreading cell death and *Botrytis* susceptibility in *bos1-*
203 *c4** and *bos1-c5** were similar to wildtype (Fig. 3D and E), indicating that these
204 exon disrupting alleles act as intragenic suppressors of *bos1-1*. Collectively,
205 these findings demonstrate that the *bos1-1* phenotypes were caused by the
206 alterations to *BOS1* function, rather than other genomic changes in *bos1-1*.

207



208

209 **Figure 4. Phenotypes of *bos1-1* are caused by *MAS* promoter driven *BOS1* expression.**

210 **(A)** Schematic diagram of the T-DNA structure in *bos1-1*. Two adjacent T-DNAs were inserted in
 211 the 5'UTR of *BOS1* with *MAS* promoters indicated in blue according to re-sequencing analysis.
 212 The red numbers indicate the insertion position of the T-DNA in *bos1-1* relative to the *BOS1* start
 213 codon.

214 **(B)** Expression profile of *BOS1* after wounding. Normalized transcript abundances of *BOS1* were
215 calculated from RNAseq data as fragments per kilobase pair of exon model per million fragments
216 mapped (FPKM). The log₂ FPKM of indicated genotypes were used to build the heatmap.

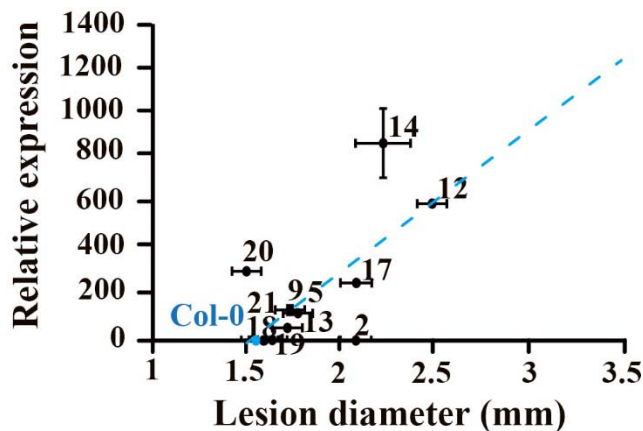
217 **(C)** RNA-seq reads mapped to *BOS1* genomic DNA. The entire coding sequence of *BOS1* was
218 expressed in *bos1-1*.

219 **(D, E)** *pMAS::BOS1* exhibited *bos1-1* mimic phenotypes upon wounding **(D)** and *Botrytis* infection
220 **(E)** treatments. **(D)** Representative pictures and quantitative data of spreading cell death induced
221 by toothpick-puncture wounds. Trypan blue staining was performed three times with similar
222 results ($n=24$ in total). Scale bar=0.5 mm. **(E)** *Botrytis* induced lesion sizes are shown in the
223 representative pictures and also as quantitative data. Statistical analysis was performed with one-
224 way ANOVA (three independent biological replicates; $n=24$ in total). All error bars represent the
225 SE of means. Letters above the bars indicate significance groups ($P<0.05$, linear mixed model).
226 Scale bar=0.5 cm.

227

228 We hypothesised that the T-DNA insertion caused altered expression of *BOS1*,
229 which conferred the cell death phenotype in *bos1-1*. The exact site of the T-DNA
230 insertion was unclear (Kraepiel et al., 2011). We used genome resequencing
231 data and Sanger sequencing, which identified two adjacent T-DNAs in opposite
232 orientations between -410 bp to -396 bp in the 5'-UTR of *BOS1* (Fig. 4A). Notably,
233 we found a *mannopine synthase* (*MAS*) promoter in the end of each T-DNA (Fig.
234 4A). The *MAS* promoter is wounding inducible and controls gene expression in a
235 bi-directional manner (Guevara-García et al., 1999). Accordingly, the expression
236 of *BOS1* in *bos1-1* was highly wounding inducible (Fig. 4B). Each side of the
237 *MAS* promoters resulted in expression of two detectable transcripts: the *BOS1*
238 mRNA with a shorter 5'-UTR that was consistent with expression driven in the T-
239 DNA and a sequence transcribed in the opposite direction derived from the T-
240 DNA (Supplemental Fig. S2). For the *BOS1* transcript, the full coding sequence
241 of *BOS1* was expressed and no alternative splicing events or mutations were
242 detected (Fig. 4C; Supplemental Fig. S2). This supports that *bos1-1* phenotypes
243 were the result of high *BOS1* transcript levels driven by the *MAS* promoter. To
244 test this hypothesis, we transformed *pMAS::BOS1* into wildtype to test if it could
245 confer *bos1-1* phenotypes. During generation of transgenic lines, many
246 *pMAS::BOS1* lines exhibited pathogen susceptible phenotypes under
247 greenhouse conditions and died after flowering (Supplemental Fig. S3). This was

248 consistent with our previous observation that *bos1-1* did not survive under
249 greenhouse conditions (Cui et al., 2019). In clean growth room experiments,
250 *pMAS::BOS1* exhibited spreading cell death upon wounding, and enhanced
251 *Botrytis* susceptibility, similar to *bos1-1* (Fig. 4D and E). Thus, the two key *bos1-1*
252 phenotypes were successfully reproduced by introduction of *pMAS::BOS1* to
253 wildtype. Overall, we conclude that *bos1-1* is a gain-of-function mutant caused by
254 *pMAS* driven expression of *BOS1*.



256

257 **Figure 5. *BOS1* transcript levels in eleven *p35S::BOS1* lines were positively correlated with**
258 ***Botrytis* susceptibility.** The relative *BOS1* expression of the eleven independent T₂
259 overexpression lines was examined by qPCR. The lesion sizes were measured as described
260 previously. Three independent biological replicates ($n \geq 48$ in total) were combined and analysed.
261 The blue dashed line indicates the correlation trend. Pearson coefficient $r = 0.72$, indicating a
262 strong correlation between *BOS1* transcript levels and lesion sizes. Raw data for this figure is
263 available in Supplemental Data Set 1.

264

265 Multiple lines of evidence support a connection between *BOS1* transcript levels
266 and *bos1-1* phenotypes: extraordinarily high *BOS1* transcript levels were
267 detected in *bos1-1* upon wounding and *Botrytis* treatments (Fig. 3C; Mengiste et
268 al., 2013). The extent of PCD propagation in *bos1-1* was positively correlated
269 with the transcript levels of *BOS1*, as *BOS1/bos1-1* had lower transcript levels of
270 *BOS1* and accordingly less cell death than *bos1-1/bos1-1* (Fig. 1C and D; Fig.
271 3C). To further confirm whether increased *BOS1* transcript levels enhance plant
272 susceptibility to *Botrytis*, we constructed a series of *BOS1* overexpression lines

273 with the 35S promoter. We challenged these lines with *Botrytis* infection and
274 found a positive correlation between lesion sizes and *BOS1* transcript levels (Fig.
275 5). This further supports that the *bos1-1* *Botrytis* susceptibility was caused by
276 increased *BOS1* transcript levels.

277 **BOS1 in abiotic stress**

278 *BOS1* transcript accumulation was elevated in response to multiple stresses
279 (Supplemental Fig. S4). In order to assess the role of *BOS1* in abiotic stress and
280 hormone responses the responses to ABA, methyl viologen, and NaCl were
281 monitored in the new loss-of-function crisper mutant alleles (Supplemental Figs.
282 S5-S7). These experiments revealed increased sensitivity to ABA in these new
283 mutant alleles (Supplemental Fig S5). However, mutant responses were
284 indistinguishable from wildtype under NaCl and methyl viologen treatments
285 (Supplemental Figs. S6-S7).

286 **Discussion**

287 **Is *bos1-1* a loss-of-function or gain-of-function allele?**

288 The inconsistent phenotypes between *bos1-1* and other *bos1* alleles were noted
289 in previous studies; *bos1-1* exhibited no reduced fertility, in stark contrast to the
290 clear reduction in fertility observed in T-DNA intron alleles (Mandaokar and
291 Browse, 2009). Conversely, *bos1* T-DNA intron alleles had no pathogen
292 phenotypes (Mandaokar and Browse, 2009; Kraepiel et al., 2011). This
293 discrepancy only stands when *bos1-1* was interpreted as a loss-of-function
294 mutant, which came about perhaps due to the limitation of technology in that time
295 and a lack of other *bos1* alleles available for confirmation of phenotypes. Our
296 data above illustrate that the cell death spread and *Botrytis* susceptibility of *bos1-*
297 *1* were conferred by altered expression of *BOS1* rather than loss-of-function of
298 *BOS1*. However, it is important to note that the original identification of *bos1-1*
299 (Mengiste et al., 2003), used several lines of evidence, which supported well that
300 *bos1-1* was a recessive loss-of-function mutant. This included genetic
301 segregation and genomic complementation analyses. Importantly, the differences

302 in procedures and conditions used in different labs may have altered the
303 phenotypes observed. Differences in growth conditions or infection protocols can
304 significantly influence the extent of *Botrytis* infection (Ciliberti et al., 2015; Harper
305 et al., 1981). The key differences between our study and Mengiste et al. include
306 fungal cultivation medium (2×V8 vs. potato dextrose broth), infection medium
307 (Sabouraud maltose broth vs. potato dextrose broth), and the age of infected
308 plants (3-weeks vs. 24-days). These differences may to some extent account for
309 the different results seen between these studies. Mengiste et al. (2003) present
310 transgenic mutant complementation data in Fig. 6C of their paper. Because of
311 the relative lesion sizes between the complemented mutant (*bos1-1 +BOS1*) and
312 *bos1-1* are much greater in comparison to that between complemented mutant
313 and wild type, Mengiste et al.(2003) considered the symptoms of the
314 complementation line as the same as wild type. However, by our own evaluation
315 of this figure, the complemented mutant line exhibited *Botrytis* symptoms that
316 were stronger than wild type, with larger lesion sizes and enhanced cell death
317 around the lesion frontiers. The choice of *Botrytis* strain may also impact the
318 extent of lesion sizes. This is well illustrated by a test of 96 diverse *Botrytis*
319 isolates that demonstrates how different *Botrytis* strains result in contrasting
320 symptoms (Zhang et al., 2017). The exact *Botrytis* strain was not specified in
321 Mengiste et al., 2003. We speculate that the fungal cultivation/infection method in
322 Megiste et al., 2003 might have led to increased contrast between the disease
323 symptoms of *bos1-1* homozygous and *bos1/BOS1* heterozygous or the
324 complementation lines, and obscured the intermediate phenotypes of the
325 heterozygote or complemented line (Mengiste et al., 2003).

326 **Increased *BOS1* transcript levels cause *Botrytis* susceptibility and**
327 **uncontained cell death**

328 Both *pMAS* and *p35S* driven expression of *BOS1* conferred *Botrytis* susceptibility,
329 but with some informative differences. While *pMAS* gave robust phenotypes, the
330 35S promoter had outcomes that were more variable (Fig. 5). The *pMAS*
331 promoter conferred strong wound inducible *BOS1* expression (Fig 4), which

332 might lead to more precise *BOS1* expression at its target tissue (infection or
333 wound sites), as compared to the general expression patterns of *p35S*. Use of
334 *p35S* can also have unintended consequences. Multiple studies have illustrated
335 gene silencing and integration site effects from gene overexpression using the
336 35S promoter (Schubert et al., 2004; Daxinger et al., 2008; Mlotshwa et al., 2010;
337 Gelvin, 2017). To further address this, eleven *p35S::BOS1* lines were examined
338 with *Botrytis* inoculation (Fig. 5). Most but not all of these overexpression lines
339 exhibited enhanced susceptibility to *Botrytis*. A previous study showed that
340 overexpression of *35S:BOS1-GUS* increased *Botrytis* resistance (Luo et al.,
341 2010). Although the possibility that the fusion of *BOS1* to *GUS* might have
342 altered the function of *BOS1* could not be excluded, it is not rare that some
343 overexpression lines may exhibit phenotypes opposite to the other lines. In our
344 study, there were also two such exceptional lines, #2 and #20, among our eleven
345 *p35S::BOS1* lines (Fig. 5). Especially, #20 had more than 300 fold increased
346 expression of *BOS1*, however showed slightly reduced lesion size (Fig. 5). This
347 demonstrates the importance of evaluating many independent overexpression
348 lines for gene function analysis.

349 **The *bos1* Crispr knock-outs and T-DNA alleles, but not *bos1-1*, have fertility** 350 **defects**

351 In unstressed condition, *BOS1* is mostly expressed in the cell types responsible
352 for anther dehiscence (Mandaokar and Browse, 2009; Xu et al., 2019).
353 Dehiscence requires properly timed PCD for pollen release (Wilson et al., 2011;
354 Beals and Goldberg, 1997; Senatore et al., 2009). Our CRISPR knock-out lines
355 exhibited alterations in the extent or timing of dehiscence, similar to *bos1* T-DNA
356 intron alleles (Fig. 2B; Mandaokar and Browse, 2009; Xu et al., 2019). This
357 suggests that *BOS1* could be required for cell death regulation in septum or
358 stomium cells of the dehiscence zone. Thereby, the roles of *BOS1* in both stress
359 responses and development could be unified as the requirement of *BOS1* for
360 proper cell death regulation. The *bos1* knock-out lines have no pathogen
361 associated phenotypes (Fig. 1C; Kraepiel et al., 2011). Only when *BOS1*

362 transcript levels are above a certain threshold, such as in *bos1-1* after *Botrytis*
363 infection, the cell death promoted by high expression of *BOS1* may result in
364 altered pathogen sensitivity. *BOS1* transcript levels were elevated during multiple
365 stresses (Supplemental Fig. S4). As this implies a role for *BOS1* in abiotic
366 defence responses, we treated *bos1-crispr* lines with ABA, NaCl and methyl
367 viologen. The *bos1-crispr* lines exhibited enhanced sensitivity to ABA while
368 unaltered sensitivity to methyl viologen and NaCl (Supplemental Figs. S5-S7).
369 Further characterization of *bos1-crispr* lines to a broader range of stress and
370 hormone treatment will help to clarify which signalling pathways are controlled by
371 this transcription factor.

372 **Summary**

373 A revaluation of previous generations of genetic tools is required (Nikonorova et
374 al., 2018). The development of gene editing technologies allows accurate
375 examination of gene function. These new tools facilitate re-evaluation of mutants
376 and a refinement of our interpretation of the scientific literature (Gao et al., 2015;
377 Westphal et al., 2008). Here, we have built upon the previous work (Mengiste et
378 al. 2003) and demonstrated the function of *BOS1* as a positive regulator of cell
379 death. Aside from our proposed changes to some of the interpretations, the
380 majority of this seminal paper still stands (Mengiste et al. 2003). Based on our
381 previous publications and results here, we propose that *BOS1* regulates cell
382 death propagation signals from dying cells to neighbour cells, rather than cell
383 death initiation. This role may be of wider interest to the plant research
384 community and warrants further investigation.

385

386 **Materials and methods**

387 ***Cultivation conditions***

388 Plant seedlings were transplanted to a mixture of peat and vermiculite (1:1) one
389 week after *in vitro* growth on ½ MS medium. Plant growth conditions were

390 23/18 °C (day/night) temperature, 120-150 $\mu\text{mol m}^{-2} \text{s}^{-2}$ light intensity, 12/12 h
391 (light/dark) photoperiod, and 60% humidity. *Botrytis* strain Bo5.10 was cultivated
392 on commercial medium of potato dextrose agar (PDA; P2182, Sigma-Aldrich,
393 USA). *Botrytis* plates were kept in dark at room temperature and transferred into
394 4°C when conidia were produced.

395 ***Infection and wounding assays***

396 Fresh *Botrytis* conidia were collected with mycelium into 1/3 strength potato
397 dextrose broth. The mixture was vortexed and filtered to remove mycelia. Conidia
398 were suspended at a concentration of 2×10^5 spores ml^{-1} . Fully expanded leaves
399 of 24-day old plants were inoculated with 3 μl conidia solution. Plants were
400 covered with a transparent plastic lid to keep 100% humidity. Symptoms were
401 photographed at 3 days post inoculation (dpi). Wounding was conducted with a
402 toothpick by puncturing fully expanded leaves of 23-day-old plants. Wounding-
403 induced cell death was visualized by trypan blue staining with wounded leaves
404 collected at 4 days post wounding (dpw). Both lesion sizes and wounding-
405 induced cell death were measured by using ImageJ (<http://rsb.info.nih.gov/ij/>).
406 The basic experimental procedures of cell death staining were the same as in our
407 previous publications (Cui et al., 2013, 2019).

408 ***Seedling growth assays***

409 For the ABA and NaCl treatments, sterilized seeds were sown on $\frac{1}{2}$ MS media
410 containing ABA or NaCl with indicated concentrations. The root lengths were
411 photographed at nine days after sowing, and measured by using ImageJ
412 (<http://rsb.info.nih.gov/ij/>). For methyl viologen treatment, seeds were germinated
413 on control plates and four-day-old seedlings were transferred to media with
414 indicated concentrations of methyl viologen. Photos were taken at 15 days after
415 transplanting.

416 ***Cloning procedures***

417 The genomic DNA of *BOS1* was cloned into the vector pGWB412 to construct

418 the p35S::*BOS1* plasmid. The *MAS* promoter was cloned with template DNA
419 from the *bos1-1* mutant, and then replaced the 35S promoter of 35S::*BOS1* to
420 create *pMAS>::BOS1*. For Crispr-Cas9 knock-out alleles, guide RNA (gRNA)
421 targeting the first and second exons of *BOS1* were integrated into
422 pCBC_DT1DT2 and then into the final vector pHEC401 according to (Xing et al.,
423 2014). Vectors were transformed into the indicated plants *via* *Agrobacterium*
424 strain GV3101. The primers used in this study are listed in Supplemental Table2.

425 ***Transformation procedures***

426 The *bos1-1* mutant is not amenable to transformation with *Agrobacterium*. The
427 *Agrobacterium* transformation of *bos1-1* was performed in labs in Helsinki,
428 Finland and Hangzhou, China. All *bos1-1* plants died before seed set because of
429 the spreading cell death triggered from *Agrobacterium* infection. To overcome this
430 limitation, our strategy was that the Crispr-Cas9 vectors were first transformed to
431 wildtype, and then introduced to *bos1-1* via crossing of *bos1-1* and the
432 transformed wildtype.

433 ***Genome re-sequencing***

434 Genomic DNA of *bos1-1* was extracted and sequenced by the Biomarker
435 Technologies Corporation (Beijing, China) following the standard procedures of
436 Oxford Nanopore Technology sequencing (Deamer et al., 2016). Sequence
437 depth was 129x, 99.77% of 24.37 Gb clean data mapped properly to the
438 *Arabidopsis* genome (TAIR10). The raw data has been deposited to NCBI
439 (PRJNA728243). Structural variations were analyzed with Sniffles (Sedlazeck et
440 al., 2018).

441 ***RNA-sequencing***

442 Fully expanded leaves of 23-day-old plants were punctured with bunched
443 toothpicks, and collected after three days. Unwounded plants were used as
444 control. RNA was extracted with TRIzol reagent (Invitrogen, Carlsbad, CA, USA),
445 library construction and sequencing were carried out in LC-BIO Bio-tech Ltd with
446 Illumina Hiseq 4000. Raw reads were filtered and aligned to the *Arabidopsis*

447 genome (TAIR10) using the hisat2 (v2.1.0) (Kim et al., 2015). To identify the
448 transcripts adjacent to *pMAS*, we first obtained the conjoined sequence of the T-
449 DNA and *BOS1* genome sequence from the *bos1-1* mutant resequencing
450 analysis, verified the sequence with Sanger sequencing, and then used the
451 combined sequence as reference for read mapping. The RNA seq raw data has
452 been deposited to NCBI (PRJNA728243). Normalized transcript abundances of
453 *BOS1* were calculated as fragments per kilobase pair of exon model per million
454 fragments mapped (FPKM) with Cufflinks (Trapnell et al., 2010). For real-time
455 quantitative PCR (qPCR), leaves of 23-day-old plants were used for RNA
456 extraction and reverse transcription. The raw cycle threshold values were
457 analyzed with Qbase+ (Biogazelle; Hellemans et al., 2007) with the reference
458 genes *Actin2*, *PP2AA3*, and *Actin8*.

459 **Statistical analysis**

460 The experiments of *Botrytis* inoculation and wounding treatments were
461 performed at least three times. Lesion sizes and cell death spread were analyzed
462 with scripts in R (version 3.0.3). Briefly, combined experiments were subjected to
463 a linear mixed model with the nlme package with fixed effect for genotypes,
464 treatments and a random effect for biological repeats. Multcomp package were
465 used to estimate the contrasts and single-step *P*-value correction were used to
466 estimate the *P*-value. Pearson coefficient calculations in R were used to support
467 the strength of correlation.

468 **Accession Numbers**

469 Gene identifiers for *Arabidopsis* *BOS1*/MYB108 (AT3G06490), *Actin2*
470 (AT3G18780), *PP2AA3* (AT1G13320), *Actin8* (AT1G49240). New sequencing
471 data, including *bos1-1* resequencing data and RNA-seq data can be found at the
472 NCBI SRA (PRJNA728243).

473 **Supplemental Data**

474 The following materials are available in the online version of this article.

475 **Supplemental Fig. S1.** Phenotype segregation in F₂ plants in response to
476 *Botrytis* infection and wounding treatments. (A) Plant symptoms induced by
477 *Botrytis* inoculation. Representative plants of known genotypes, which were
478 determined by PCR. Bar = 1 cm. (B-C) The number of F₂ *bos1-1/Col-0*
479 individuals exhibiting the indicated symptoms upon *Botrytis*- (B) and wounding-
480 (C) treatments. The genotypes of several plants were confirmed by PCR and are
481 presented as representative symptoms. F₂ individuals with similar symptoms
482 were counted and the number of individuals in each category are listed. A model
483 with a co-dominant effect for *bos1-1* was used as the null hypothesis for the χ^2 -
484 test.

485 **Supplemental Fig. S2.** Illustration of the transcripts at the *BOS1* loci in *bos1-1*
486 mutant.

487 **Supplemental Fig. S3.** Photos of *pMAS::BOS1* lines grown in greenhouse.

488 **Supplemental Fig. S4.** *BOS1* transcript levels in publicly available *Arabidopsis*
489 RNAseq data. The Genevestigator perturbation tool was used to identify
490 experiments with highest up-regulation of *BOS1* transcript levels (Hruz et al.,
491 2008). The identification number for each experiment refers to the identifier in the
492 Genevestigator database.

493 **Supplemental Fig. S5.** The *bos1-crispr* loss-of-function mutants exhibited
494 enhanced ABA sensitivity. (A-B) Symptoms of the plants in response to ABA at
495 the indicated concentrations. These experiments were repeated twice with similar
496 results. Bar = 1 cm. (C) Pooled quantitative data of the root lengths of two
497 independent biological repeats. Stars indicated the significant different groups (p
498 < 0.05; *t*-test)

499 **Supplemental Fig. S6.** The *bos1-crispr* loss-of-function mutants exhibited
500 unaltered sensitivity to methyl viologen. (A) Illustration of the plant genotypes (B-
501 D) Symptoms of the plants in response to methyl viologen at the indicated
502 concentrations. These experiments were repeated twice with similar results and
503 one representative experiment is shown. Bar = 1 cm.

504 **Supplemental Fig. S7.** The *bos1*-crispr loss-of-function mutants exhibited
505 unaltered NaCl sensitivity. The root length of the indicated genotypes were
506 measured on the 9th day. These experiments were repeated twice with similar
507 results (n=20 in total). Stars indicate the groups that are significantly different (p
508 < 0.05; *t*-test).

509 **Supplemental Table S1:** Identification of genomic changes in *bos1-1*, identified
510 through genome re-sequencing.

511 **Supplemental Table S2:** Primers used in this study.

512 **Supplemental Data Set 1:** Raw data for Figure 5, including lesion sizes and
513 *BOS1* transcript levels.

514 **Acknowledgments**

515 This work supported by the Natural Science Foundation of Zhejiang Province
516 (grant no. LY22C160005); the National Natural Science Foundation of China
517 (grant no. 31700224 and 31871233); No conflict of interest declared.

518 **References**

- 519 **Beals, T.P. and Goldberg, R.B.** (1997). A novel cell ablation strategy blocks tobacco anther
520 dehiscence. *Plant Cell* **9**: 1527–1545.
- 521 **Bostock, R.M. and Stermer, B.A.** (1989). Perspectives on wound healing in resistance to
522 pathogens. *Annu. Rev. Phytopathol.* **27**: 343–371.
- 523 **Brown, C.G. and Clarke, J.** (2016). Nanopore development at Oxford Nanopore. *Nat. Biotechnol.*
524 **34**: 810–811.
- 525 **Bruggeman, Q., Raynaud, C., Benhamed, M., and Delarue, M.** (2015). To die or not to die?
526 Lessons from lesion mimic mutants. *Front. Plant Sci.* **6**: 24. doi: 10.3389/fpls.2015.00024.
- 527 **Ciliberti, N., Fermaud, M., Roudet, J., and Rossi, V.** (2015). Environmental Conditions Affect
528 *Botrytis cinerea* Infection of Mature Grape Berries More Than the Strain or Transposon
529 Genotype. *Phytopathology*® **105**: 1090–1096.
- 530 **Cui, F., Brosché, M., Sipari, N., Tang, S., and Overmyer, K.** (2013). Regulation of ABA
531 dependent wound induced spreading cell death by MYB108. *New Phytol.* **200**: 634–640.
- 532 **Cui, F., Wu, W., Wang, K., Zhang, Y., Hu, Z., Brosché, M., Liu, S., and Overmyer, K.** (2019).
533 Cell death regulation but not abscisic acid signaling is required for enhanced immunity to
534 *Botrytis* in *Arabidopsis* cuticle-permeable mutants. *J. Ex. Bot.* **70**: 5971–5984.

- 535 **Daneva, A., Gao, Z., Van Durme, M., and Nowack, M.K.** (2016). Functions and Regulation of
536 Programmed Cell Death in Plant Development. *Annual Review of Cell and*
537 *Developmental Biology* **32**: 441–468.
- 538 **Daxinger, L., Hunter, B., Sheikh, M., Jauvion, V., Gascioli, V., Vaucheret, H., Matzke, M.,**
539 **and Furner, I.** (2008). Unexpected silencing effects from T-DNA tags in Arabidopsis.
540 *Trends in Plant Science* **13**: 4–6.
- 541 **Deamer, D., Akeson, M., and Branton, D.** (2016). Three decades of nanopore sequencing. *Nat.*
542 *Biotechnol.* **34**: 518–524.
- 543 **Gao, Y., Zhang, Y., Zhang, D., Dai, X., Estelle, M., and Zhao, Y.** (2015). Auxin binding protein 1
544 (ABP1) is not required for either auxin signaling or Arabidopsis development. *Proc. Natl.*
545 *Acad. Sci. USA* **112**: 2275–2280.
- 546 **Gelvin, S.B.** (2017). Integration of Agrobacterium T-DNA into the Plant Genome. *Annual Review*
547 *of Genetics* **51**: 195–217.
- 548 **Guevara-García, A., López-Bucio, J., and Herrera-Estrella, L.** (1999). The mannopine
549 synthase promoter contains vectorial cis-regulatory elements that act as enhancers and
550 silencers. *Mol. Gen. Genet.* **262**: 608–617.
- 551 **Harper, A.M., Strange, R.N., and Langcake, P.** (1981). Characterization of the nutrients
552 required by *Botrytis cinerea* to infect broad bean leaves. *Physiological Plant Pathology* **19**:
553 153–167.
- 554 **Hellemans, J., Mortier, G., De Paepe, A., Speleman, F., and Vandesompele, J.** (2007). qBase
555 relative quantification framework and software for management and automated analysis
556 of real-time quantitative PCR data. *Genome Biol.* **8**: R19. doi: 10.1186/gb-2007-8-2-r19
- 557 **Hruz, T., Laule, O., Szabo, G., Wessendorp, F., Bleuler, S., Oertle, L., Widmayer, P.,**
558 **Gruissem, W., and Zimmermann, P.** (2008). Genevestigator v3: a reference expression
559 database for the meta-analysis of transcriptomes. *Adv Bioinformatics* **2008**: 420747.
- 560 **Huysmans, M., Lema A, S., Coll, N.S., and Nowack, M.K.** (2017). Dying two deaths —
561 programmed cell death regulation in development and disease. *Current Opinion in Plant*
562 *Biology* **35**: 37–44.
- 563 **Lakimova, E.T. and Woltering, E.J.** (2018). The wound response in fresh-cut lettuce involves
564 programmed cell death events. *Protoplasma* **255**: 1225–1238.
- 565 **Jiang, W., Zhou, H., Bi, H., Fromm, M., Yang, B., and Weeks, D.P.** (2013). Demonstration of
566 CRISPR/Cas9/sgRNA-mediated targeted gene modification in Arabidopsis, tobacco,
567 sorghum and rice. *Nucleic Acids Res.* **41**.
- 568 **Jupe, F., Rivkin, A.C., Michael, T.P., Zander, M., Motley, S.T., Sandoval, J.P., Slotkin, R.K.,**
569 **Chen, H., Castanon, R., Nery, J.R., and Ecker, J.R.** (2019). The complex architecture
570 and epigenomic impact of plant T-DNA insertions. *PLoS Genet.* **15**: e1007819.
- 571 **Kim, D., Langmead, B., and Salzberg, S.L.** (2015). HISAT: a fast spliced aligner with low
572 memory requirements. *Nat. Methods* **12**: 357–360.
- 573 **Kraepiel, Y., Pédrón, J., Patrit, O., Simond-Côte, E., Hermand, V., and Van Gijsegem, F.**
574 (2011). Analysis of the plant *bos1* mutant highlights necrosis as an efficient defence
575 mechanism during *D. dadantii/Arabidopsis thaliana* interaction. *PLoS One* **6**: e18991.

- 576 **Lorrain, S., Vaillau, F., Balagué, C., and Roby, D.** (2003). Lesion mimic mutants: keys for
577 deciphering cell death and defense pathways in plants? *Trends in Plant Sci.* **8**: 263–271.
- 578 **Luo, H., Laluk, K., Lai, Z., Veronese, P., Song, F., and Mengiste, T.** (2010). The Arabidopsis
579 Botrytis susceptible1 interactor defines a subclass of RING E3 ligases that regulate
580 pathogen and stress responses. *Plant Physiol.* **154**: 1766–1782.
- 581 **Mandaokar, A. and Browse, J.** (2009). MYB108 acts together with MYB24 to regulate
582 jasmonate-mediated stamen maturation in Arabidopsis. *Plant Physiol* **149**: 851–862.
- 583 **McCabe, P.F.** (2013). Healing and closure following death: death signals from a wounded leaf.
584 *New Phytol.* **200**: 590–591.
- 585 **Mengiste, T., Chen, X., Salmeron, J., and Dietrich, R.** (2003). The *BOTRYTIS SUSCEPTIBLE1*
586 gene encodes an R2R3MYB transcription factor protein that is required for biotic and
587 abiotic stress responses in Arabidopsis. *Plant Cell* **15**: 2551–2565.
- 588 **Mlotshwa, S., Pruss, G.J., Gao, Z., Mgutshini, N.L., Li, J., Chen, X., Bowman, L.H., and**
589 **Vance, V.** (2010). Transcriptional silencing induced by Arabidopsis T-DNA mutants is
590 associated with 35S promoter siRNAs and requires genes involved in siRNA-mediated
591 chromatin silencing. *The Plant Journal* **64**: 699–704.
- 592 **Nikonorova, N., Yue, K., Beeckman, T., and De Smet, I.** (2018). Arabidopsis research requires
593 a critical re-evaluation of genetic tools. *Journal of Experimental Botany* **69**: 3541–3544.
- 594 **Schubert, D., Lechtenberg, B., Forsbach, A., Gils, M., Bahadur, S., and Schmidt, R.** (2004).
595 Silencing in Arabidopsis T-DNA Transformants: The Predominant Role of a Gene-
596 Specific RNA Sensing Mechanism versus Position Effects. *The Plant Cell* **16**: 2561–2572.
- 597 **Sedlazeck, F.J., Rescheneder, P., Smolka, M., Fang, H., Nattestad, M., von Haeseler, A., and**
598 **Schatz, M.C.** (2018). Accurate detection of complex structural variations using single-
599 molecule sequencing. *Nat. Methods* **15**: 461–468.
- 600 **Senatore, A., Trobacher, C.P., and Greenwood, J.S.** (2009). Ricinosomes predict programmed
601 cell death leading to anther dehiscence in tomato. *Plant Physiol.* **149**: 775–790.
- 602 **Trapnell, C., Williams, B.A., Pertea, G., Mortazavi, A., Kwan, G., van Baren, M.J., Salzberg,**
603 **S.L., Wold, B.J., and Pachter, L.** (2010). Transcript assembly and abundance
604 estimation from RNA-Seq reveals thousands of new transcripts and switching among
605 isoforms. *Nat. Biotechnol.* **28**: 511–515.
- 606 **Van Hautegeem, T., Waters, A.J., Goodrich, J., and Nowack, M.K.** (2015). Only in dying, life:
607 programmed cell death during plant development. *Trends Plant Sci.* **20**: 102–113.
- 608 **Westphal, L., Scheel, D., and Rosahl, S.** (2008). The *coi1-16* mutant harbors a second site
609 mutation rendering PEN2 nonfunctional. *Plant Cell* **20**: 824–826.
- 610 **Wilson, Z.A., Song, J., Taylor, B., and Yang, C.** (2011). The final split: the regulation of anther
611 dehiscence. *J. Ex. Bot.* **62**: 1633–1649.
- 612 **Xing, H.-L., Dong, L., Wang, Z.-P., Zhang, H.-Y., Han, C.-Y., Liu, B., Wang, X.-C., and Chen,**
613 **Q.-J.** (2014). A CRISPR/Cas9 toolkit for multiplex genome editing in plants. *BMC Plant*
614 *Biol.* **14**: 327.

615 **Xu, X.-F., Wang, B., Feng, Y.-F., Xue, J.-S., Qian, X.-X., Liu, S.-Q., Zhou, J., Yu, Y.-H., Yang,**
616 **N.-Y., Xu, P., and Yang, Z.-N.** (2019). AUXIN RESPONSE FACTOR17 directly regulates
617 *MYB108* for anther dehiscence. *Plant Physiol.* **181**: 645–655.

618 **Zhang, W., Corwin, J.A., Copeland, D., Feusier, J., Eshbaugh, R., Chen, F., Atwell, S., and**
619 **Kliebenstein, D.J.** (2017). Plastic Transcriptomes Stabilize Immunity to Pathogen
620 Diversity: The Jasmonic Acid and Salicylic Acid Networks within the Arabidopsis/Botrytis
621 Pathosystem. *The Plant Cell* 29: 2727–2752.

622

623




624 Supplemental Figures

625 Fig S1.

A






B

Symptom			
Genotype	WT	<i>bos1-1</i>	<i>bos1-1/BOS1</i>
Replicate1	12	11	26
Replicate2	16	14	29
Total (observed)	28	25	55
Expected	27	27	54

$\chi^2 = 0.2037$, $df=2$; $\chi^2 < 5.99$, null hypothesis can not be rejected

C

Symptom			
Genotype	WT	<i>bos1-1</i>	<i>bos1-1/BOS1</i>
Replicate1	11	12	25
Replicate2	19	16	32
Total (observed)	30	28	57
Expected	28.75	28.75	57.5

626 $\chi^2 = 0.0783$, $df=2$; $\chi^2 < 5.99$, null hypothesis can not be rejected

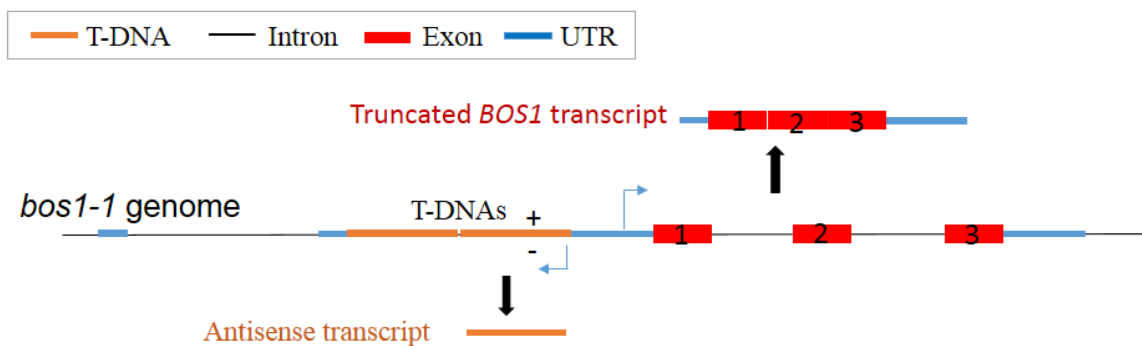
627 **Supplemental Figure S1.** Phenotype segregation in F₂ plants in response to *Botrytis*
 628 infection and wounding treatments. (A) Plant symptoms induced by *Botrytis* inoculation.
 629 Representative plants of known genotypes, which were confirmed by PCR. Bar = 1 cm.

630 (B-C) The number of F₂ *bos1-1*/Col-0 individuals exhibiting the indicated symptoms
631 upon *Botrytis*- (B) and wounding- (C) treatments. The genotypes of several plants were
632 confirmed by PCR and are presented as representative symptoms. F₂ individuals with
633 similar symptoms were counted and the number of individuals in each category are
634 listed. A model with a co-dominant effect of *bos1-1* was used as the null hypothesis for
635 the χ^2 -test.

636 Fig. S2

637 >Antisense_transcript

638 TCAGGACTTTTTTTTTTTTTTTTTTTTTAGGAA TTA GAAATTTTATTGATAGAAATTTTTACAATAACAAATACATACTAAGGGTTTCTTATATGC
 639 TCAACACATGAGCGAAACCTATAAGAACCCTAATTCCTTATCTGGGAACTACTCACACATTATTATAGAGAGAGATAGATTGTAGAGAGAGACT
 640 GGTGATTTACAGCGGGCATGCCTGCAGGTCGACTCTAGAGGATCTAGAACCGTGATCTCAGATCTCGGTGACGGGCGAGGACCGGACGGGGCGG
 641 TACCGGCAGGCTGAAGTCAGCTGCCAGAAACCCAGTCATGCCAGTTCCCGTGCTGAAGCCGGCCGCCCGCAGCATGCCGCGGGGGGCATATC
 642 CGAGCGCTCTGTCATGCGCACGCTCGGGTCTTTGGGACGCCGATGACAGCGACCAACCGCTTTGAAGCCCTGTGCCTCCAGGGAATTCAGCAGG
 643 TGGGTGTAGAGCGTGGAGCCAGTCCCGTCCGCTGTTGGCGGGGGAGACGTACACGGTCTGACTCGGCCGTCCAGTCTAGGCGTTGCGTGCCT
 644 TCCAGGGGCCCGGTAGGCGATGCCGGCGACCTCGCGTCCACTCGGCGACGAGCCAGGGATAGCGCTCCCGACACGGACGAGGTGCTCCGT
 645 CCACTCCTGCGGTTCTGCGGCTCGGTACGGAAGTTGACCGTCTTGTCTCGATGTAGTGTTGACGATGGTGCAGACCGCCGGCATGTCCGCCTC
 646 GGTGGCACGGCGGATGTCGGCCGGGCGTCTTGGGCTCATGGATCCAGTGTGGAAGATATGAATTTTTGAGAACTAGATAAGATTAATG
 647 AATATCGGTGTTTGGTTTTCTTTGTGGCCGCTTTGTTTATATTGAGATTTTCAAATCAGTGGCGCAAGACGTGACGTAAGTATCCGAGTCAGTTT
 648 TTATTTTCTACTAATTTGTCGTTTATTTCCGCGTGTAGGACATGCAACCGGGCTGAATTTCCGCGGTA TTCTGTTTCTATCCAATTTTTCTTG
 649 ATCCGCAGCCATTAACGACTTTTGAATAGATACGCTGACACGCCAAGCCTCGCTAGTCAAAAGTGTA CCAAACAACGCTTTACAGCAAGAACGGAA
 650 TCGCGTGTGACGCTCGCGGTGACGCCATTTGCGCTTTT CAGAAATGGATAAATAGCCTTGCTTCTATTATA TCTTCCAAATTACCAATAATTACAC
 651 TAGCATCTGAATTTCAATCAATCTCGATACACCAATCGAATTCATTCGCGGTTAATTCAGTACATTAATAAATCGTCCGCAATGTGTTAATGTT
 652 GTCTAAGCGTCAATTTGTTTACCAACAAATTTGTGGACAAATTT
 653



654

655

656 >*BOS1*_transcript

657 CGGCTGTCTATTCCTTCATCGCACATGTTCCAATAATTTAAAAA TAAAAA GAAAAATTGAAAACTACTCTCTTTTTCTTCTATAAAACCCACAA
 658 CTTCTCTTTTTCTGTGCATTCAAAACATCCTCTATCTCTATCTACATAACTCCAAAAACAAACAAATTTCTCTCTATCTCTCTTCGAAAAACAA
 659 CATAGAAAAAAGTAGAAAGTCTCAATCTTTTGTCTGAAACAATCTGTTGTGGTCTCTTCTGTGTATATCAATGGATGAAAAAGGAA GAAGCTTGAA
 660 GAACAACAACATGGAAGA CGAGATGGACCTAAAGAGAGGTCCTGGACTGCTGAAGAAGATTTAAGCTCATGAAATTAATTGCTACTAATGGAG
 661 AAGGTCGCTGGAACCTCTTTCTCGTTGCGCGGCCTCAACGCAACGGTAAAAGCTGTAGACTAAGGTGGTTAACTATCTCCGCCCTGACGTCCG
 662 CCGTGGAACATTACACTGAAGAACAACTTTGATCTCGAACTTCATTCCTGTTGGGAAATAGATGGTCAAAAAATCGCACAATATTTA CCGGGA
 663 AGAACGGACAACGAGATCAAGAACTA CTGGAGGACGCGGGTGC AAAAGCATGCGAAACAGTTGAAATGTGATGTGAATAGCCAACAATTCAAAG
 664 ACACAATGAAGTACTTGTGGATGCCTCGACTAGTCGAGAGGATTCAATCAGCTCGGCTCATCCGACGAGCAGCCACCACCACAACACCACCA
 665 CCACAGGATCAGCCGGCAGTCACTTTGCATCA CAA CCTCTAACAAATCAA TTCATGAATTAAGACTACAACAACAA CAATGGGACAACAGTTTGG
 666 TGTAATGAGCAACAATGATTATATCA CGCCTGAAAA TTCCAGCGTGGCAGTGTCTCCGGCTGAGACTTAACGGAGTACTACAGCGCTCCAAACCC
 667 TAACCCGGAATACTATTCGGGTCAAATGGGGAATAGTTATTATCCAGATCAGAAATTTAGTGAATTCACAATTAATACCGGATAATTTTCGACTAT
 668 AGTGGATTATTAGACGAAGATCTAACGGCTATGCAAGAGCAGAGTAACCTCAGCTGGTTTAAAA CATTAAATGGTGCTGCTTCTCTCAGACGTT
 669 TATGGAACATTGGAGAACTGATGAAGAATCTGGTTCTTACAGCAGCAACAACAGTTCAACAATAATGGTAGCTTCTGAAGTTAGAAAAA
 670 TAGAAATCGTTTTAAGTTAAATTATCACTATAGTATACGTGTGAAAGGAATTTGTTGTAAGGGAATAATTAATAAATAAAGAAATTTGTTTCATAGGATA
 671 TATGATCAGGTTTTTATACCAAGCTTGATCATATATCATGGCGTTTTAACAAAGCGCTAAAATTGATTGGTTTTGTTTTGGGGGGGATTGCAATG
 672 ATATTTTGGATAAATGATAAATTTGGATGAAATAATTTATGATTAATGTTTGGAAAAATACTCATTCTCGGTGGGACTATGTATACTATAAACA
 673 TAAATAATGGAAATTTGATTACACTATAGATTGAGTGATTTCCCTCAATGGAAGCATAATATAAAAA CATTATTCATTTAAAAAAGAA
 674
 675

676

677

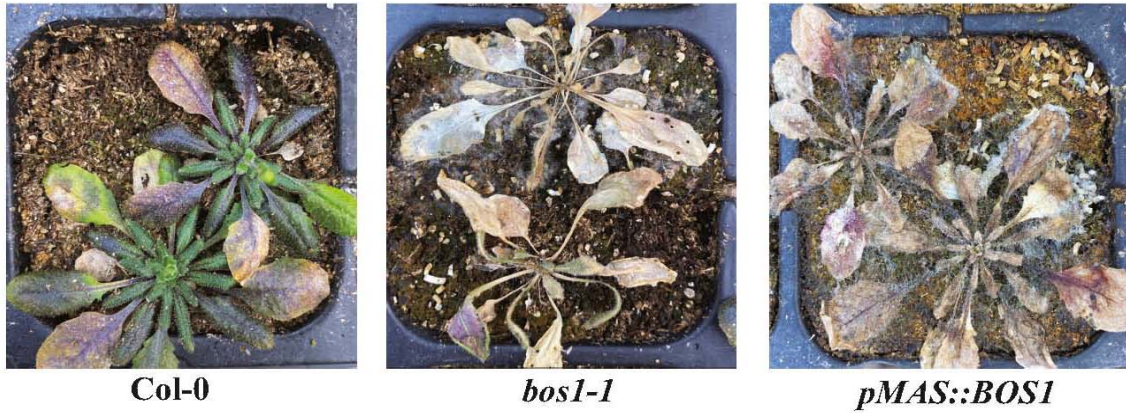
678 **Supplemental Figure S2.** Illustration of the transcripts at the *BOS1* locus in *bos1-1*
 679 mutant. Two transcripts were found in the RNA-seq analysis. One is the truncated *BOS1*
 680 transcript with a shorter 5'-UTR, and the other is an antisense transcript from the T-DNA.

681

682

681 Fig. S3

682



684

685

686 **Supplemental Figure S3.** The *pMAS: BOS1* lines were more sensitive to pathogens
687 under standard greenhouse conditions. Plants grown in the greenhouse without
688 fungicide application. Many *pMAS: BOS1* lines were infected and died before setting
689 seed. Representative plants of the indicated genotypes are shown.

690

691

691 Fig. S4

692

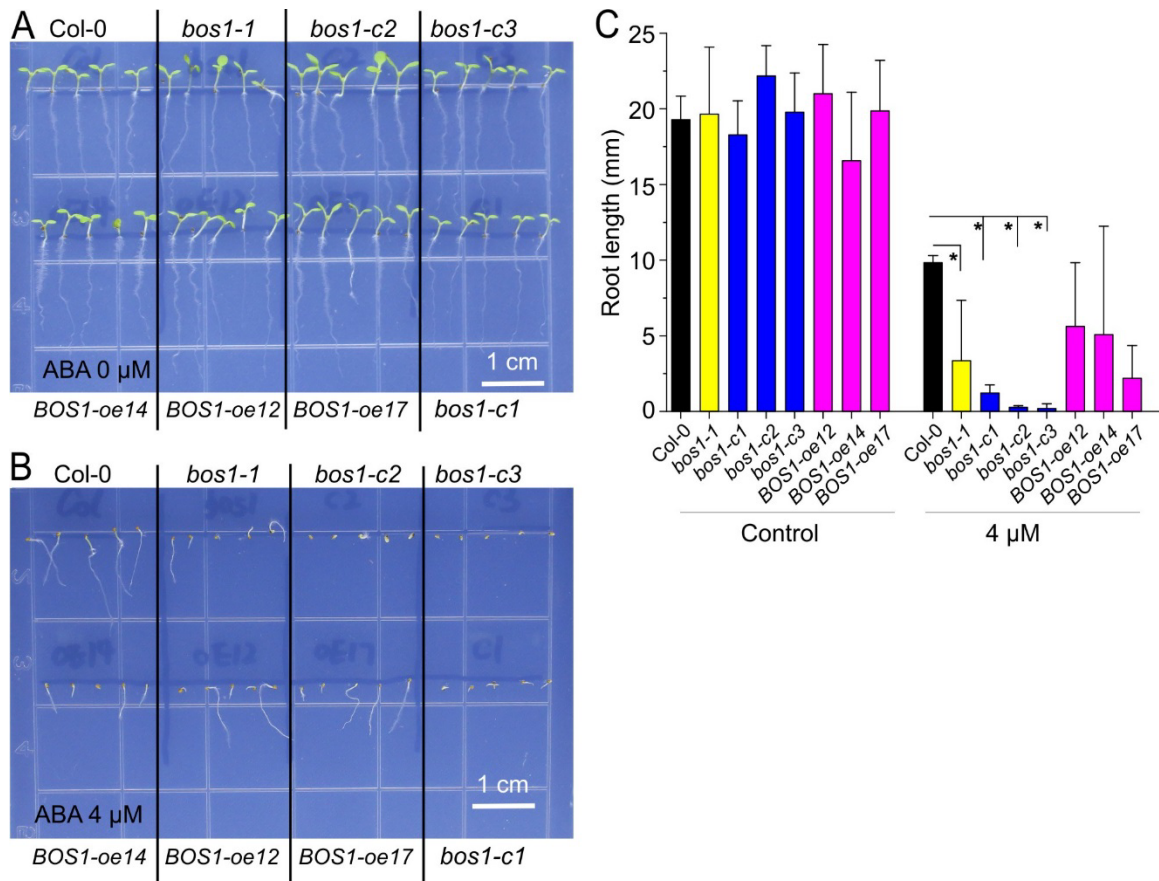


693

694 **Supplemental Figure S4.** *BOS1* transcript levels in publicly available Arabidopsis
695 RNAseq data. The Genevestigator perturbation tool was used to identify experiments
696 with highest up-regulation of *BOS1* transcript levels (Hruz et al., 2008). The identification
697 number for each experiment refers to the identifier in the Genevestigator database.

698 Fig. S5

699

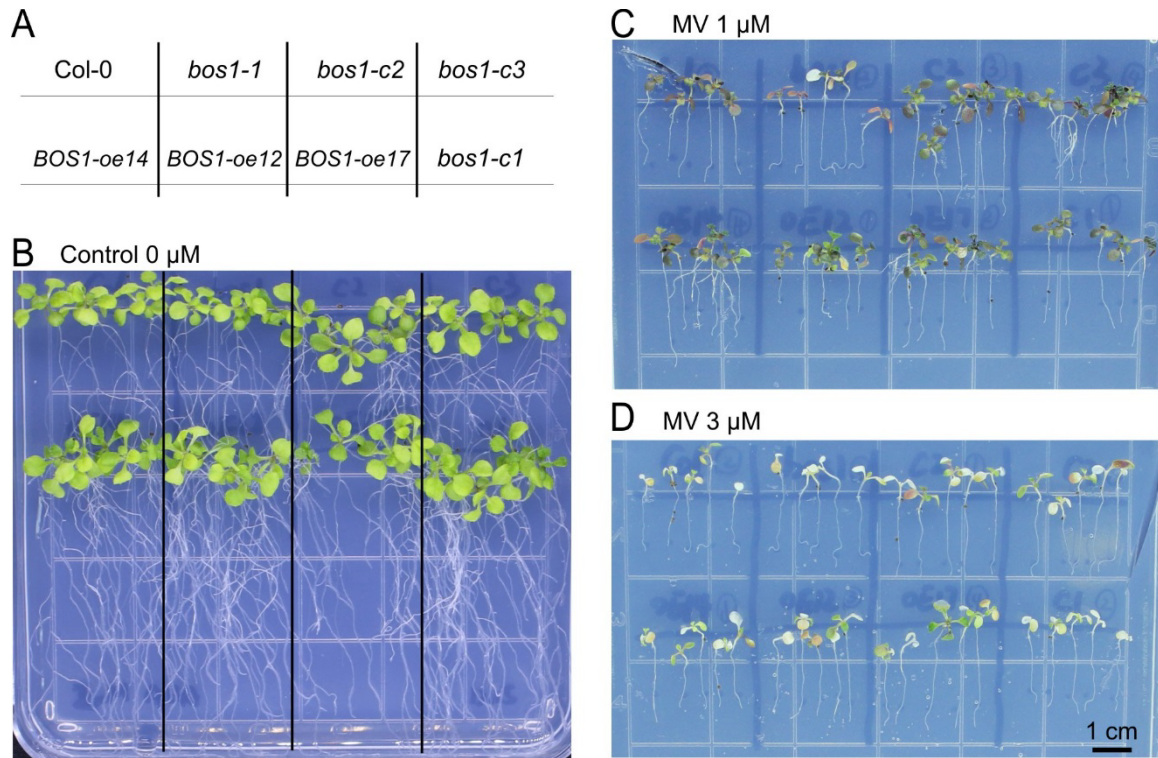


700

701 **Supplemental Figure S5.** The *bos1-crispr* loss-of-function mutants exhibited enhanced
702 ABA sensitivity. (A-B) Symptoms of the plants in response to ABA at the indicated
703 concentrations. These experiments were repeated twice with similar results. Bar = 1 cm.
704 (C) Pooled quantitative data of the root lengths of two independent biological repeats.
705 Stars indicated the significant different groups (p < 0.05; *t*-test).

706 Fig. S6

707



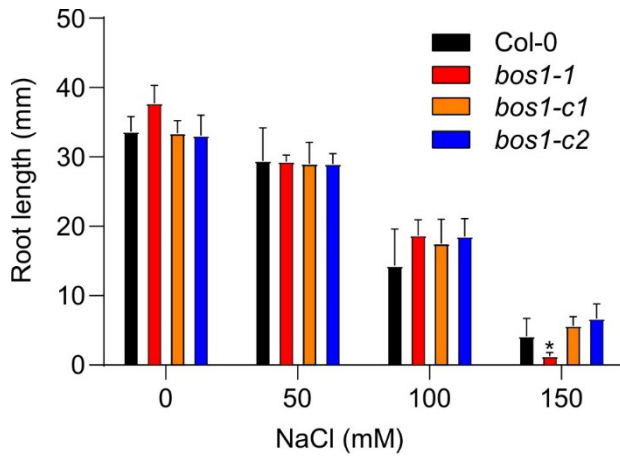
708

709

710 **Supplemental Figure S6.** The *bos1*-crispr loss-of-function mutants exhibited unaltered
711 sensitivity to methyl viologen. (A) Illustration of the plant genotypes (B-D) Symptoms of
712 the plants in response to methyl viologen at the indicated concentrations. These
713 experiments were repeated twice with similar results and one representative experiment
714 is shown. Bar = 1 cm.

715 Fig. S7

716



717

718 **Supplemental Figure S7.** The *bos1*-crispr loss-of-function mutants exhibited unaltered
719 NaCl sensitivity. The root length of the indicated genotypes were measured on the 9th
720 day. These experiments were repeated twice with similar results (n=20 in total). Stars
721 indicate the groups that are significantly different ($p < 0.05$; *t*-test).